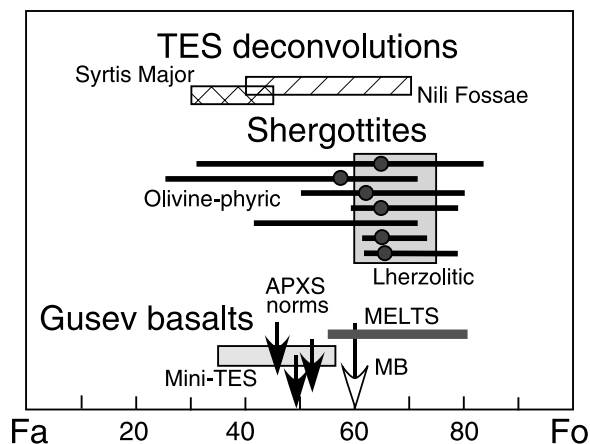


(a) Olivine Compositions



(b) Olivine Proportions

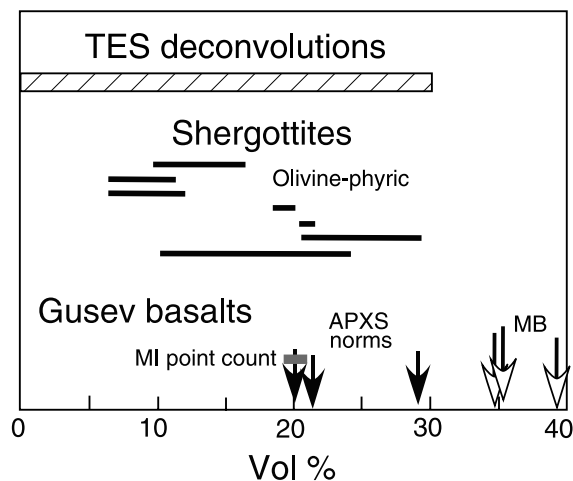


Figure 11. (a) Comparison of olivine compositions (mol% forsterite Mg_2SiO_4) for Adirondack, Humphrey, and Mazatzal measured by MiniTES and Mössbauer (MB) spectroscopy and APXS normative calculations with electron probe analyses for olivines in olivine-phyric and lherzolithic shergottites (references in Table 2). The shaded circles on olivine-phyric shergottite range bars are the normative olivine compositions for those meteorites (Table 2). The bar labeled MELTS represents the range of olivine compositions predicted to crystallize from Gusev basalt magmas (see text). Also shown are the ranges of olivine compositions determined from orbital TES spectra [Hoefen *et al.*, 2003; Hamilton *et al.*, 2003]. (b) Comparison of olivine abundances in Adirondack, Humphrey, and Mazatzal with point-counts of olivine-phyric shergottites (Table 2; ranges reflect counts of multiple thin sections) and olivine abundances estimated from TES spectra [Hoefen *et al.*, 2003].

dominantly in associated spinel (also an early crystallizing phase; see section 6.1) rather than being hosted in olivine.

[36] The tight clustering of Gusev basalt compositions may provide a further argument that the olivines they contain are phenocrysts. Incorporation of xenocrysts or cumulates would likely be a random process, producing

Table 2. Properties of Olivine in Olivine-Phyric Shergottites

| Meteorite | Compositional Range, % Fo | Abundance, vol% | Normative Composition, ^a % Fo | References ^b |
|----------------------|---------------------------|-----------------|--|-------------------------|
| Dho 019 | 72-25 | 7-12 | 57 | (1) |
| EETA 79001 | 81-52 | 7-13 | 62 | (2), (3) |
| DaG 476 ^c | 79-62 | 10-24 | 66 | (4-7) |
| DaG 489 ^c | 79-59 | 18-20 | 66 | (6), (8) |
| SAU 005 | 74-62 | 21-29 | 65 | (9) |
| NWA 1068 | 72-42 | 21 | | (10) |
| Y-980459 | 84-31 | 9-16 | 65 | (11-14) |

^aNorm calculations assume $Fe^{2+}/Fe(\text{total}) = 0.84$, as in Humphrey [Morris *et al.*, 2004].

^bReferences: (1) Taylor *et al.* [2002], (2) Steele and Smith [1982], (3) McSween and Jarosewich [1983], (4) Zipfel *et al.* [2000], (5) Mikouchi *et al.* [2001], (6) Wadhwa *et al.* [2001], (7) Koizumi *et al.* [2004], (8) Folco *et al.* [2000], (9) Goodrich [2003], (10) Barrat *et al.* [2002], (11) Greshake *et al.* [2004], (12) Ikeda [2004], (13) Mikouchi *et al.* [2004], (14) Shirai and Ebihara [2004].

^cProbably paired, along with DaG 670, 735, 876, 975.

^dNo silica analysis reported, so norm cannot be calculated.

variable proportions of megacrysts and varying bulk rock chemistry. Despite apparent differences in modal olivine contents in Adirondack, Humphrey, and Mazatzal, their chemical compositions are nearly uniform.

5.2. Orbital Spectroscopy and Regional/Global Context

[37] The Thermal Emission Spectrometer (TES) on Mars Global Surveyor has provided unprecedented insights into the composition of broad areas of the Martian surface. A detailed study of atmospherically corrected spectra [Smith *et al.*, 2000] in Cimmeria Terra by Christensen *et al.* [2000] identified basaltic surface compositions dominated by plagioclase (45% and 53%) and high-calcium pyroxene (26% and 19%) with detectable amounts of olivine (12%). Further analyses [Hoefen *et al.*, 2003; Hamilton and Christensen, 2005] of TES spectra using several intermediate olivine

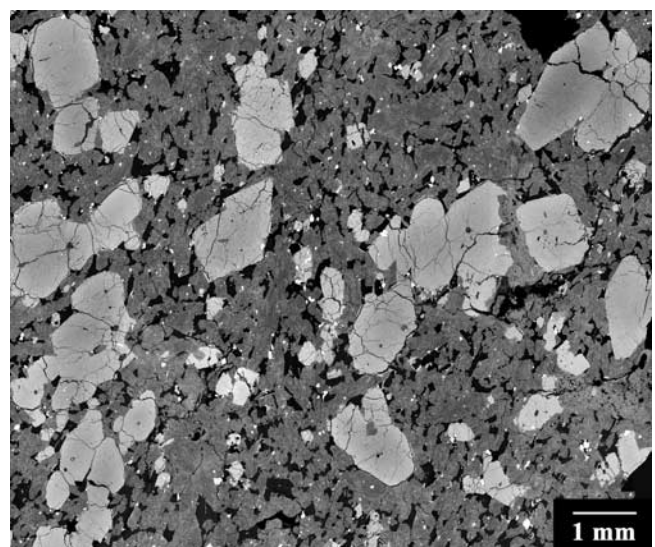


Figure 12. Backscattered electron (BSE) image of olivine-phyric shergottite SAU 005 showing olivine megacrysts in a groundmass of pyroxenes and plagioclase. Figure is 5.5 mm across [after Goodrich, 2003].